This article was downloaded by: [Institute Of Atmospheric Physics]
On: 09 December 2014, At: 15:24
Publisher: Taylor & Francis
Informa Ltd Registered in England and Wales Registered Number: 1072954 Registered office: Mortimer House, 37-41 Mortimer Street, London W1T 3JH, UK

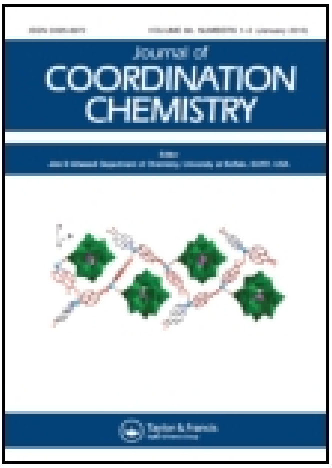

Click for updates

Journal of Coordination Chemistry
Publication details, including instructions for authors and subscription information:
http://www.tandfonline.com/loi/gcoo20

Eco-friendly energetic complexes based on transition metal nitrates and 3,4-diamino-1,2,4-triazole (DATr)

Xin Jin[a], Jian-Guo Zhang[a], Cai-Xia Xu[a], Xin Yin[a], Piao He[a] & Qian Qin[a]
[a] State Key Laboratory of Explosion Science and Technology, Beijing Institute of Technology, Beijing, China

Accepted author version posted online: 08 Sep 2014.Published online: 23 Sep 2014.

To cite this article: Xin Jin, Jian-Guo Zhang, Cai-Xia Xu, Xin Yin, Piao He & Qian Qin (2014) Eco-friendly energetic complexes based on transition metal nitrates and 3,4-diamino-1,2,4-triazole (DATr), Journal of Coordination Chemistry, 67:19, 3202-3215, DOI: 10.1080/00958972.2014.960862

To link to this article: http://dx.doi.org/10.1080/00958972.2014.960862

PLEASE SCROLL DOWN FOR ARTICLE

Taylor & Francis makes every effort to ensure the accuracy of all the information (the "Content") contained in the publications on our platform. However, Taylor & Francis, our agents, and our licensors make no representations or warranties whatsoever as to the accuracy, completeness, or suitability for any purpose of the Content. Any opinions and views expressed in this publication are the opinions and views of the authors, and are not the views of or endorsed by Taylor & Francis. The accuracy of the Content should not be relied upon and should be independently verified with primary sources of information. Taylor and Francis shall not be liable for any losses, actions, claims, proceedings, demands, costs, expenses, damages, and other liabilities whatsoever or howsoever caused arising directly or indirectly in connection with, in relation to or arising out of the use of the Content.

This article may be used for research, teaching, and private study purposes. Any substantial or systematic reproduction, redistribution, reselling, loan, sub-licensing, systematic supply, or distribution in any form to anyone is expressly forbidden. Terms &

Journal of Coordination Chemistry, 2014
Vol. 67, No. 19, 3202–3215, http://dx.doi.org/10.1080/00958972.2014.960862

Eco-friendly energetic complexes based on transition metal nitrates and 3,4-diamino-1,2,4-triazole (DATr)

XIN JIN, JIAN-GUO ZHANG*, CAI-XIA XU, XIN YIN, PIAO HE and QIAN QIN

State Key Laboratory of Explosion Science and Technology, Beijing Institute of Technology, Beijing, China

(*Received 16 May 2014; accepted 24 July 2014*)

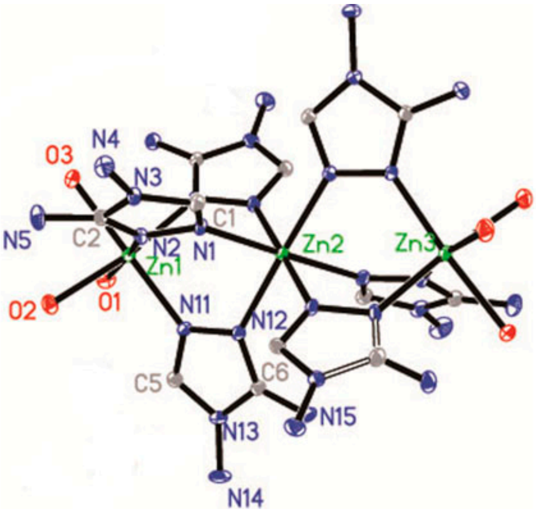

Four nitrate-containing metal complexes based on 3,4-diamino-1,2,4-triazole are described as eco-friendly energetic coordination compounds. Their synthesis, characterization, and some energetic properties are studied. The figure reveals the crystal structure of zinc (II) complex and also suggests the coordination mode of metal complexes.

Four eco-friendly energetic metal complexes of 3,4-diamino-1,2,4-triazole (DATr), including manganese (**1**), cobalt (**2**), nickel (**3**), and zinc (**4**), were synthesized by reacting DATr·HCl with the corresponding metal (Mn(II), Co(II), Ni(II), and Zn(II)) nitrate in aqueous solution and characterized by using Fourier transform-infrared spectroscopy and elemental analyses. The single crystals of **2**, **3**, and **4** were obtained and determined by X-ray single-crystal diffraction analysis. All three complexes crystallize in the *monoclinic* crystal system and belong to *P2(1)/n* space group. The thermal decomposition processes were investigated by differential scanning calorimeter (DSC) and thermogravimetry–derivative thermogravimetry analyses. The results show that the decomposition temperatures of **1**–**4** are above 260 °C, depending upon their onset DSC peaks. It can be predicted that these complexes based on 3,4-diamino-1,2,4-triazole have good thermal stability. The nonisothermal kinetic parameters of decomposition were calculated by using Kissinger and Ozawa–Doyle's methods.

---

*Corresponding author. Email: zjgbit@bit.edu.cn

Furthermore, the sensitivities of these complexes to impact, friction, and flame were determined. Sensitivity tests revealed that **2** was more sensitive to external stimuli compared to the other three complexes.

Keywords: Energetic complexes; 3,4-Diamino-1,2,4-triazole; Crystal structure; Thermal decomposition; Sensitivity

1. Introduction

Recently, many researchers are investigating green energetic materials [1–4]. Considerable attention has been drawn to nontoxic metal coordination compounds based on nitrogen-rich heterocyclic groups [5–11], owing to their multiple structures [12, 13], and energetic properties. Nitrogen-rich heterocyclic compounds are mainly azole-based compounds, such as triazoles [6, 14–17], tetrazoles [4, 18–22], and their derivatives [3, 13, 23–30]. Azole compounds have some attractive energetic properties such as positive heat of formation and thermal stability characteristics [15, 31–34]. Its positive heat of formation is attributed to the existence of inherently energetic N–N and C–N bonds. Therefore, energetic complexes based on nitrogen-rich ligands and transition metal cations have some advantages, such as (1) insensitive to external stimuli; (2) thermally stable to at least 200 °C; and (3) chemically stable during long periods.

Energetic complexes, using 4-amino-1,2,4-triazole (4-AT) [6, 35, 36], 1,5-diaminotetrazole (DAT) [7, 32, 37, 38], and 3,5-diamino-1,2,4-triazole (Hdatrz) [39] neutral molecules as ligands, have been studied. The good examples of coordination compounds with polymeric tetrakis (4-AT) copper(II) perchlorate monohydrate [35], $[Cd(4\text{-}AT)_2(H_2O)_4](PA)_2$ (PA = picrate) [36], $[Co(DAT)_6](ClO_4)_2$ [40], and $Zn(DAT)_2(Ac)_2$ (Ac = acetate) [32] were reported and characterized. Besides, the complex $[Ni_3(Hdatrz)_6(fma)_2(H_2O)_4]fma \cdot 11H_2O$ (fma = fumarate) [39] was synthesized. The sensitivities towards external stimuli of these complexes are lower than that of common primary explosives, such as lead azide [41], so it is believed that energetic complexes based on nitrogen-rich ligands are insensitive to external stimuli. Meanwhile, from the mentioned compounds and the present work, it is known that late-transition metal of group 7–12 elements are used as central ions. However, compared to 4-AT, 3,4-diamino-1,2,4-triazole (DATr) contains an additional amino group. Therefore, DATr as ligand not only improves the nitrogen content and coordination ability, but also enhances the possibility of hydrogen bonds. As a result, it modifies the performances.

3,4-Diamino-1,2,4-triazole (DATr) as a ligand has rarely been researched. DATr has high content of nitrogen (70.67 wt%) in which the nitrogens have lone pair electrons, so it is possible to coordinate with the central metal ions [40]. Due to DATr and its derivatives as ligands forming stable complexes with various structures, they show excellent characteristics in transition metal complexes.

The π-system and N–H groups of DATr will benefit for the formation of intermolecular hydrogen bonds as nonclassic acceptors and donors of protons [42, 43]. Moreover, the existence of a 3-D network of hydrogen bonds increases the stability of complexes [42].

DATr can be coordinated as a monodentate ligand using $-NH_2$ group or triazole ring, while as bridging ligands using N1 and N2 of triazole ring can link metal ions. Synthesis and preparation of $Zn(DATr)_2Cl_2$ have been reported previously [44]. But complexes with transition metal as central ions and DATr as energetic ligands have still been seldom reported. In order to research new energetic coordination compounds for eco-friendly environment without heavy metals and free perchlorates, four complexes which use nontoxic transition metal (Mn, Co, Ni, and Zn) as cations with DATr and nitrate anions have been synthesized. We report crystal structures, thermal decomposition, and energetic properties of such complexes in the present work.

2. Experimental

2.1. *Materials and general methods*

Caution: The title complexes are potential energetic materials that tend to explode under certain conditions. Although we experienced no difficulties during the preparation and handling of the complexes, they are still energetic materials. Proper protective measures (leather coat, safety glasses, face shields, and ear plugs) should be taken, especially when the complexes are prepared on a large scale.

All the reagents and solvents were of analytical grade and used without purification as commercially obtained. 3,4-Diamino-1,2,4-triazole was prepared according to a literature method [45].

Elemental analyses were performed with a Flash EA 1112 full-automatic trace element analyzer. The Fourier transform-infrared (FT-IR) spectra were recorded with a Bruker Equinox 55 infrared spectrometer (KBr pellets) from 4000 to 400 cm^{-1} with a resolution of 4 cm^{-1}. Differential scanning calorimeter (DSC) and TG measurements were carried out with a Pyris-1 DSC and Pyris-1 thermo-gravimetric analyzer (Perkin-Elmer, USA) in a dry nitrogen gas atmosphere with flowing rate of 20 mL min^{-1}.

2.2. *Syntheses*

Silver carbonate (6.89 g) was dissolved in distilled water (20 mL) and nitric acid (3.45 mL, 65%) was slowly added dropwise into it. They were then added to a solution of DATr·HCl (6.78 g) in water (50 mL) and stirred for 10 min, and then were placed to precipitate completely in the dark. Afterwards filtering the mixtures, the pH of the filtrate was adjusted to neutral. The $M(NO_3)_2$ (M = Mn, Co, Ni, and Zn) (25 mM) was added slowly to the filtrate and stirred for 30 min. Finally the suspension was cooled. The precipitate was filtered off and dried in medium vacuum.

2.2.1. $Mn_3[(DATr)_6(H_2O)_6](NO_3)_6\cdot 2H_2O$ (1). The white powder of 1 was gained, but Mn complex's crystal was not obtained. Yield: 12.68% (1.31 g, 1.06 mM). Elemental analysis Calcd (%) for $C_{12}H_{46}N_{36}O_{26}Mn_3$: C, 11.29; H, 3.61; N, 39.51. Found: C, 11.40; H, 3.72; N, 39.59. IR (KBr, cm^{-1}): $\tilde{\nu}$ = 3467(s), 3310(s), 2374(m), 1652(s), 1560(w), 1355(s), 1209(m), 1003(s), 825(s), 728(s), 681(w), 636(s), 504(s).

2.2.2. $Co_3[(DATr)_6(H_2O)_6](NO_3)_6\cdot 2H_2O$ (2). After a few days, the brick-red product started to crystallize. Yield: 15.38% (1.65 g, 1.28 mM). Elemental analysis Calcd (%) for $C_{12}H_{46}N_{36}O_{26}Co_3$: C, 11.19; H, 3.60; N, 39.16. Found: C, 11.17; H, 3.64; N, 39.13. IR

(KBr, cm^{-1}): $\tilde{\nu}$ = 3328(s), 2249(m), 1650(s), 1536(w), 1356(s), 1041(s), 827(s), 727(s), 682 (w), 639(s), 509(w).

2.2.3. $Ni_3[(DATr)_6(H_2O)_6](NO_3)_6{\cdot}1.5H_2O$ (3).

A couple of days later, the blue crystals of nickel complex were obtained. Yield: 49.63% (5.32 g, 4.13 mM). Elemental analysis Calcd (%) for $C_{12}H_{45}N_{36}O_{25.50}Ni_3$: C, 11.28; H, 3.61; N, 39.22. Found: C, 11.61; H, 3.40; N, 37.26. IR (KBr, cm^{-1}): $\tilde{\nu}$ = 3330(s), 2431(m), 1650(s), 1565(w), 1356(s), 1046(s), 996(s), 828(s), 726(s), 685(w), 641(s), 516(w).

2.2.4. $Zn_3[(DATr)_6(H_2O)_6](NO_3)_6{\cdot}2H_2O$ (4).

Colorless crystals suitable for X-ray analysis were obtained after several days. Yield: 21.85% (2.38 g, 1.82 mM). Elemental analysis Calcd (%) for $C_{12}H_{46}N_{36}O_{26}Zn_3$: C, 11.03; H, 3.55; N, 39.46. Found: C, 11.09; H, 3.50; N, 39.54. IR (KBr, cm^{-1}): $\tilde{\nu}$ = 3315(s), 2396(m), 1654(s), 1560(w), 1383(s), 1121(m), 1023(s), 827(s), 728(s), 682(w), 637(s), 508(m).

3. Results and discussion

3.1. *Crystal structures*

Single crystals of **2**, **3**, and **4** were obtained and determined by single-crystal X-ray diffraction. Crystallographic data are described in table 1, and selected bond lengths and angles are listed in tables 2 and 3, respectively.

Table 1. Crystallographic data and structure refinement for **2**, **3**, and **4**.

Complex	**2**	**3**	**4**
Formula	$C_{12}H_{46}N_{36}O_{26}Co_3$	$C_{12}H_{45}N_{36}O_{25.5}Ni_3$	$C_{12}H_{46}N_{36}O_{26}Zn_3$
Mr (g M^{-1})	1287.64	1277.97	1306.96
Crystal system	Monoclinic	Monoclinic	Monoclinic
Space group	*P2(1)/n*	*P2(1)/n*	*P2(1)/n*
a (Å)	10.679(2)	10.7035(5)	10.653(2)
b (Å)	22.180(3)	21.8884(9)	22.269(4)
c (Å)	19.976(4)	19.8478(8)	20.005(4)
β (°)	102.155(2)	102.319(4)	101.954(3)
V (Å^3)	4625.3(14)	4542.9(3)	4642.9(15)
Z	4	4	4
ρ (g cm^{-3})	1.849	1.869	1.870
μ (mm^{-1})	1.189	1.357	1.663
F (0 0 0)	2636	2628	2672
T (K)	153(2)	293(2)	153(2)
θ range (°)	2.7–28	2.69–25.02	2.01–29.00
Data-set (h,k,l)	$-13 \le h \le 14$, $-29 \le k \le 19$, $-26 \le l \le -13$	$-12 \le h \le 12$, $-19 \le k \le 26$, $-23 \le l \le 22$	$-14 \le h \le 13$, $-30 \le k \le 30$, $-27 \le l \le 27$
R_{int}	0.0381	0.0572	0.0438
R_1 (obsd)	0.0698	0.0834	0.0538
Max (trans)	0.7554	0.9230	0.6911
Min (trans)	0.6641	0.953	0.5216

Table 2. Selected bond lengths (Å) for **2**, **3**, and **4**.

Complex **2**		Complex **3**		Complex **4**	
Bond		Bond		Bond	
Co(1)–N(2)	2.093(3)	Ni(1)–N(3)	2.049(4)	Zn(1)–N(2)	2.100(2)
Co(1)–N(7)	2.094(3)	Ni(1)–N(8)	2.063(4)	Zn(1)–N(7)	2.102(2)
Co(1)–N(11)	2.101(3)	Ni(1)–N(13)	2.043(4)	Zn(1)–N(11)	2.099(2)
Co(1)–O(1)	2.105(3)	Ni(1)–O(1)	2.092(4)	Zn(1)–O(1)	2.136(2)
Co(1)–O(2)	2.124(3)	Ni(1)–O(2)	2.085(4)	Zn(1)–O(2)	2.160(2)
Co(1)–O(3)	2.137(3)	Ni(1)–O(3)	2.102(4)	Zn(1)–O(3)	2.152(2)
Co(2)–N(1)	2.131(3)	Ni(2)–N(2)	2.093(4)	Zn(2)–N(1)	2.140(2)
Co(2)–N(6)	2.137(3)	Ni(2)–N(7)	2.082(4)	Zn(2)–N(6)	2.155(2)
Co(2)–N(12)	2.137(3)	Ni(2)–N(12)	2.099(4)	Zn(2)–N(12)	2.167(2)
Co(2)–N(26)	2.139(3)	Ni(2)–N(17)	2.106(5)	Zn(2)–N(26)	2.180(2)
Co(2)–N(16)	2.142(3)	Ni(2)–N(22)	2.094(4)	Zn(2)–N(16)	2.176(2)
Co(2)–N(21)	2.157(3)	Ni(1)–N(27)	2.105(4)	Zn(2)–N(21)	2.183(2)
N(1)–C(1)	1.307(5)	N(1)–C(1)	1.361(7)	N(1)–C(1)	1.298(4)
N(1)–N(2)	1.402(4)	N(2)–N(3)	1.398(6)	N(1)–N(2)	1.399(3)
N(2)–C(2)	1.325(5)	N(2)–C(2)	1.294(7)	N(2)–C(2)	1.328(4)
N(3)–N(4)	1.401(5)	N (1)–N(5)	1.396(8)	N(3)–N(4)	1.408(3)
N(3)–C(2)	1.361(5)	N(3)–C(1)	1.329(8)	N(3)–C(2)	1.357(4)
N(3)–C(1)	1.360(5)	N(1)–C(2)	1.350(9)	N(3)–C(1)	1.359(4)
N(5)–C(2)	1.342(5)	N(4)–C(1)	1.342(8)	N(5)–C(2)	1.345(4)

Table 3. Selected bond angles (°) for **2**, **3**, and **4**.

Complex **2**		Complex **3**		Complex **4**	
Angle		Angle		Angle	
N(2)–Co(1)–N(7)	93.59(12)	N(3)–Ni(1)–N(8)	93.22(17)	N(2)–Zn(1)–N(7)	95.25(9)
N(7)–Co(1)–N(11)	91.66(12)	N(8)–Ni(1)–N(13)	92.14(17)	N(11)–Zn(1)–N(7)	93.40(9)
N(2)–Co(1)–O(3)	92.37(12)	N(3)–Ni(1)–O(1)	86.47(17)	N(2)–Zn(1)–O(3)	92.04(9)
N(2)–Co(1)–O(2)	87.00(12)	N(13)–Ni(1)–O(2)	87.51(17)	N(2)–Zn(1)–O(2)	86.25(9)
N(2)–Co(1)–O(1)	173.26(13)	N(3)–Ni(1)–O(3)	175.24(17)	N(2)–Zn(1)–O(1)	171.24(10)
N(7)–Co(1)–O(2)	175.05(13)	N(8)–Ni(1)–O(2)	173.52(16)	N(7)–Zn(1)–O(2)	172.24(9)
N(11)–Co(1)–O(2)	93.23(12)	N(3)–Ni(1)–O(2)	93.26(17)	N(11)–Zn(1)–O(2)	94.12(9)
N(11)–Co(1)–O(3)	175.53(12)	N(13)–Ni(1)–O(1)	175.66(18)	N(11)–Zn(1)–O(3)	174.32(9)
O(1)–Co(1)–O(2)	86.35(12)	O(1)–Ni(1)–O(2)	88.46(17)	O(1)–Zn(1)–O(2)	84.99(9)
C(2)–N(3)–N(4)	124.0(3)	C(2)–N(1)–N(5)	129.8(5)	C(2)–N(3)–N(4)	123.3(2)
C(2)–N(2)–N(1)	106.3(3)	C(2)–N(2)–N(3)	107.2(4)	C(2)–N(2)–N(1)	106.7(2)
N(2)–C(2)–N(5)	128.4(4)	N(3)–C(1)–N(4)	128.5(5)	N(2)–C(2)–N(5)	128.3(3)
N(1)–Co(2)–N(12)	90.90(12)	N(2)–Ni(2)–N(7)	89.39(17)	N(1)–Zn(2)–N(12)	91.47(9)
N(1)–Co(2)–N(16)	89.48(12)	N(2)–Ni(2)–N(12)	90.57(16)	N(1)–Zn(2)–N(16)	89.20(9)
N(12)–Co(2)–N(26)	90.10(12)	N(7)–Ni(2)–N(27)	89.51(17)	N(12)–Zn(2)–N(26)	89.54(9)
N(6)–Co(2)–N(26)	178.77(12)	N(7)–Ni(2)–N(17)	178.33(18)	N(6)–Zn(2)–N(26)	179.00(9)
N(12)–Co(2)–N(16)	178.68(12)	N(12)–Ni(2)–N(22)	179.24(17)	N(12)–Zn(2)–N(16)	178.20(9)
N(1)–Co(2)–N(21)	178.54(13)	N(17)–Ni(2)–N(27)	91.89(18)	N(1)–Zn(2)–N(21)	178.81(10)
N(6)–Co(2)–N(12)	90.24(12)	N(12)–Ni(2)–N(27)	90.03(16)	N(6)–Zn(2)–N(12)	90.56(9)

2, **3**, and **4** crystallize in the space group *P2(1)/n* with four molecular moieties in the unit cell, but the calculated densities of complex cobalt and zinc at 153(2) K are 1.849 and 1.870 g cm^{-3}, respectively, while nickel complex at 293(2) K is 1.869 g cm^{-3}. The preferred geometries of the three complexes consist of trinuclear units. Three complexes have similar structures, but **3** is slightly different from **2** and **4**, due to lack of half of the water molecules. The molecular structures and the packing diagrams of **2**, **3**, and **4** are shown in figures 1–3, respectively.

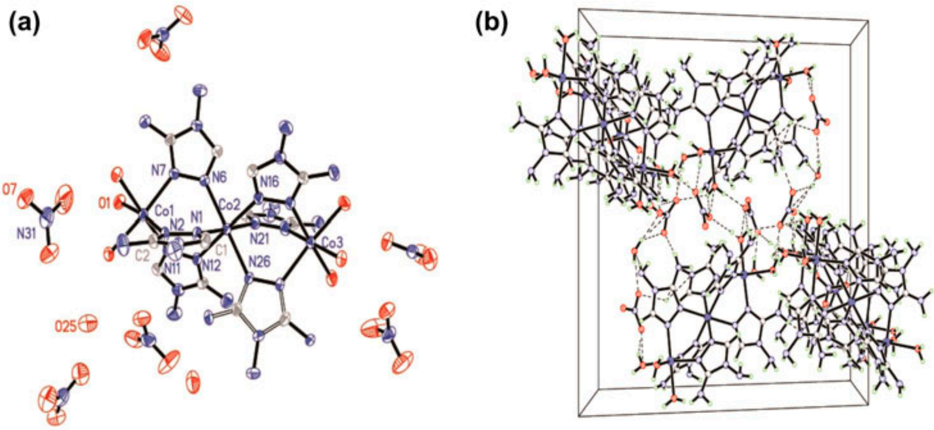

Figure 1. Molecular structure (a) and packing diagram (b) viewed down the *a*-axis of **2**.

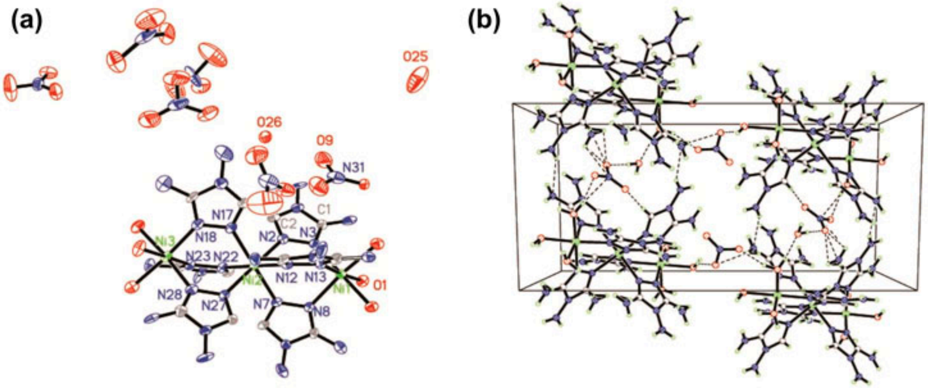

Figure 2. Molecular structure (a) and packing diagram (b) viewed down the *c*-axis of **3**.

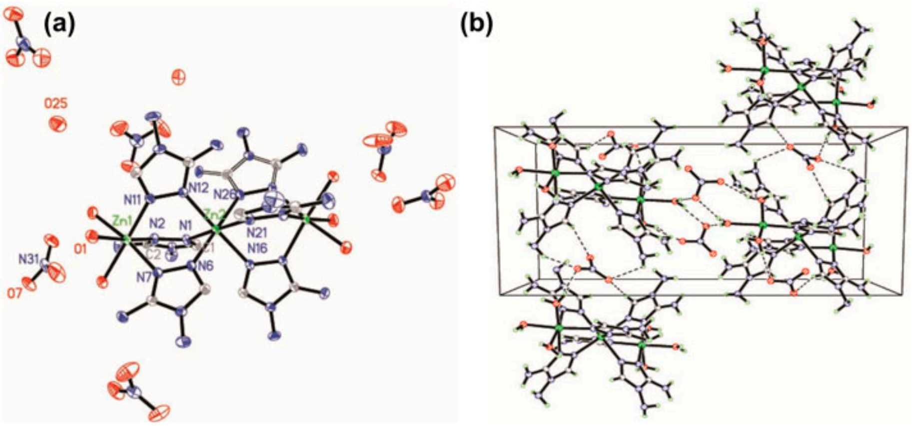

Figure 3. Molecular structure (a) and packing diagram (b) viewed down the *a*-axis of **4**.

Each metal (Co, Ni, and Zn) of three complexes shows a distorted octahedral coordination sphere due to Jahn–Teller effect, but the coordination environments around M (M = Co, Ni and Zn) ions are different. M(1) and M(3) are coordinated by three N atoms from different triazole ligands through M–N and three O atoms from different H_2O molecules through M–O, whereas six nitrogens of bridging triazole ligands coordinate the center atom M(2). The skeleton structures of **2**, **3**, and **4** are surrounded with nitrates and water molecules. In the three complexes, DATr exhibits bridging modes to link two metal ions. In general, the neighboring donors that are easy to coordinate are situated in the five-membered ring [35]. It is observed that the N1, N2 of the triazole rings are following the principle. In the basic unit, all the neighboring metal ions (Co(II), Ni(II), and Zn(II)) of trinuclear species are bridged by 3,4-diamino-1,2,4-triazole ligands.

In **2**, the distances of Co–N bonds are 2.067(4)–2.157(3) Å, while the distances of bond between cobalt and oxygen range from 2.094(3) to 2.155(3) Å. The bond lengths of cobalt atom and oxygen atoms of three water molecules are obviously different from each other (2.105(3) Å for Co(1)–O(1), 2.124(3) Å for Co(1)–O(2), and 2.137(3) Å for Co(1)–O(3)). The coordination around cobalt cation is described as a distorted octahedron because of the angles of N–Co–O and N–Co–N found in the crystal deviating from 180°.

From the packing diagram of **2**, due to the existence of the N–H and O–H, a number of hydrogen bonds including both intermolecular and intramolecular can be found in **2** [figure 1(b)]. Intermolecular hydrogen-bond contact, on which the crystal packing mainly depends, occurs among the coordinated water molecules, the oxygen atoms of nitrate anions, the crystal water molecules and the amino groups of the DATr molecules. But intramolecular hydrogen bonds are observed between oxygens of the crystal H_2O molecules, and the nitrogens of triazole rings. A 3-D supermolecular framework is formed as shown in figure 1(b), which makes an important contribution to enhance the thermal stability of the cobalt complex.

In **3**, the bond lengths of Ni–O and Ni–N are between 2.082(4) and 2.115(4) Å, between 2.037(5) and 2.106(5) Å, respectively. The angles of bond between two contra-positioned nitrogen atoms and nickel atoms as well as the angles of O–Ni–N (the nitrogens of coordinated triazole ring) deviate from 180°, which results in the distorted octahedral configuration. The torsion angle of Ni1–N3–C1–N4 is nearly 0° (2.2(10)°), which suggests that Ni1 atom and the triazole ring (the bridging DATr of N2 and N3 atoms) are coplanar.

It is observed from the packing diagram of **3** [figure 2(b)] that many intramolecular and intermolecular hydrogen bonds exist, owing to the presence of π-system and NH_2 groups of DATr ligands. Intramolecular hydrogen bonds contain various forms, for example, H–O···H (the oxygen of the crystal water and the hydrogen of coordinated water, respectively). However, formations of intermolecular hydrogen bonds mainly depend on O and N of nitrate anions. Dozens of hydrogen bonds form the 3-D structure, which contributes to the stability of **3**.

In **4**, the distances of Zn–N and Zn–O are between 2.075(3) and 2.183(2) Å, between 2.103(2) and 2.193(2) Å, respectively. The C(1)–N(1) bond length is 1.298(4) Å, which is close to C=N double bond (1.28 Å), and the C(1)–N(3) bond length is 1.359(4) Å, which indicates that the bond can be a C–N single bond (1.46 Å). The bond angles of the nitrogens from two contra-positioned triazole ligands and the Zn(II) cation are close to 180° (N(6)–Zn(2)–N(26) = 179.00(9)°, N(12)–Zn(2)–N(16) = 178.20(9)°, N(1)–Zn(2)–N(21) = 178.81(10)°). But the angle between the Zn(II) cation and the nitrogens of triazole ring, the contra-positioned oxygens of the crystal water molecules, respectively, deviate from 180° (N(2)–Zn(1)–O(1) = 171.24(10)°, N(11)–Zn(1)–O(3) = 174.32(9)°, and N(7)–Zn(1)–O(2) = 172.24(9)°), which contributes to form a slightly distorted octahedral configuration.

The packing diagram of **4** is more complicated, which is shown in figure 3(b). Extensive hydrogen bonds of intermolecular and intramolecular exist in the structure. The oxygens of NO_3^- can form hydrogen bonds through linking hydrogens of triazole rings, $-NH_2$ groups, and the crystal water molecules, respectively. Moreover, a bifurcated hydrogen interaction takes place on the coordinated water molecules (H–O···H (the hydrogens of $-NH_2$ groups), O–H···O (the oxygens of nitrate anions)). Nevertheless, intramolecular hydrogen bonds are found between hydrogens of H_2O and oxygens of NO_3^-. Large quantities of hydrogen bonds not only play an important role in strengthening the stability of the molecules, but also contribute to the formation of interesting structures.

3.2. *Thermal decomposition*

The thermal decomposition processes of the four complexes have been investigated by using DSC and thermogravimetry–derivative thermogravimetry (TG–DTG) technologies. The DSC and TG-DTG curves with the heating rate of 10 °C $\min^{-1}$ are shown in figures 4 and 5, respectively. The decomposition temperatures of **1–4** are above 260 °C based on their onset DSC peaks, and these complexes based on 3,4-diamino-1,2,4-triazole have good thermal stability.

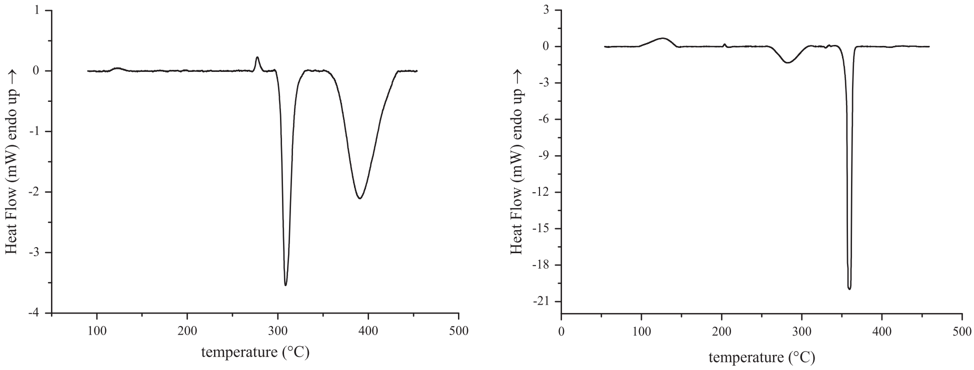

(a) Complex **1** (b) Complex **2**

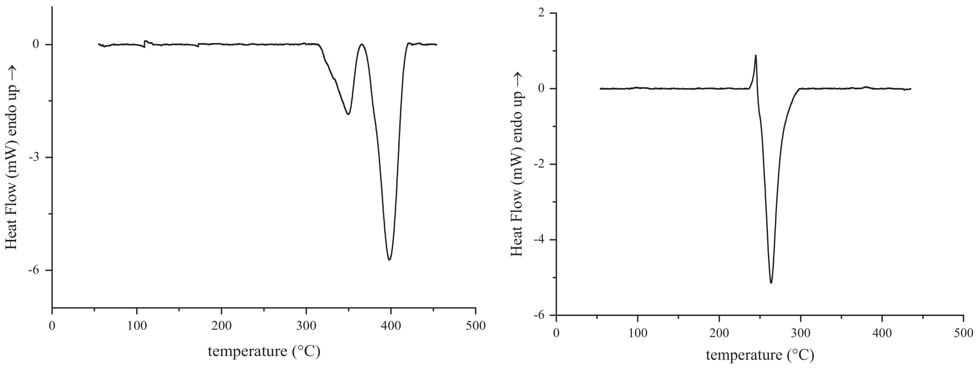

(c) Complex **3** (d) Complex **4**

Figure 4. The DSC curves of **1–4** of DATr with the heating rate of 10 °C $\min^{-1}$.

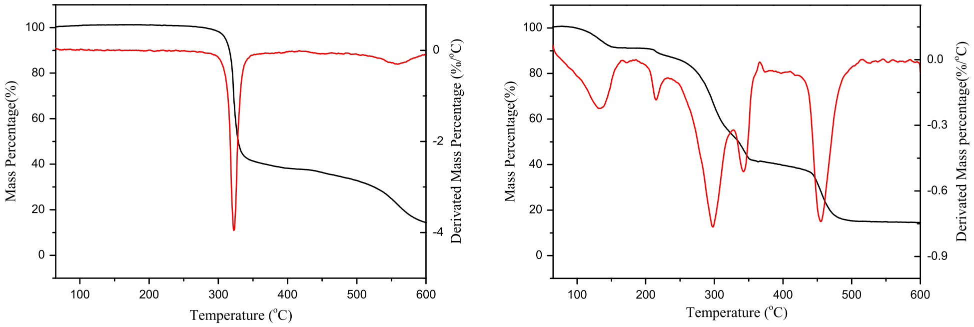

(a) Complex **1** (b) Complex **2**

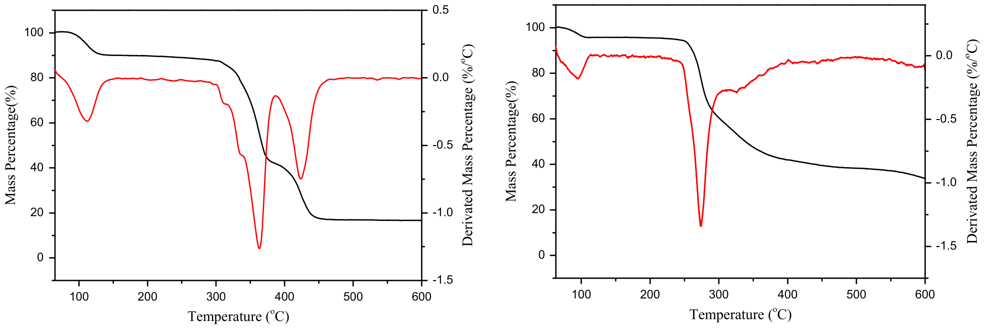

(c) Complex **3** (d) Complex **4**

Figure 5. The TG-DTG curves of 1–4 with the heating rate of 10 °C min^{-1}.

For **1**, it was found in the DSC curve that a main endothermic process with peak temperatures of 277.5 °C, and two exothermic stages with the corresponding peak temperature of 308.7 and 391.3 °C, respectively, appeared. DSC curve of **1** showed that a relatively small endothermic process occurred at 110–140 °C, which suggested that the coordination compound of Mn may contain H_2O molecules, consistent with the other three complexes. The TG-DTG curve revealed that the mass loss mainly divided into two stages including reaching the largest rate at 322.5 °C with a mass loss percentage of 61.1 and at 577.9 °C with a very small mass loss, respectively.

For **2**, small and a sharp exothermic decomposition stages during which the peak temperature commenced at 282.3 and 359.7 °C, respectively, were seen in the DSC curve. The temperature of beginning decomposition was 260.1 °C, and the TG-DTG curve showed the first mass loss process in the range from 115 to 145 °C, which reached the largest rate at 131.2 °C with a mass loss percentage of 8.6, and it denotes that some of crystal water was lost. At last, the final residue at 700 °C is 16.5%, which is coincident with the calculated value of CoO (17.5%).

For **3**, in the DSC curve, there were two successive exothermic processes with the peak temperatures of 349.9 and 398.1 °C, respectively. Mass loss observed from the TG-DTG curve was obvious. In the first stage, mass loss occurred from 100 to 130 °C, indicating crystal water could be lost. Following are second stage and the third stage at 210–390 °C, 390–470 °C, the largest mass loss percentage was 32.0% min^{-1} at 361.1 °C, 25.9% min^{-1} at 423.8 °C, respectively. In the end, the mass of the final residue is 16.6%, which may be nickel oxide (calculated value 17.5%).

The DSC curve of **4** had an endothermic process with peak temperatures of 245.1 °C, during which phase transformation can happen in the range of 235–250 °C, and an exothermic process was observed with peak temperatures of 263.9 °C. The TG-DTG curve demonstrated that the first process of mass loss occurred from 85 to 105 °C, which may be due to loss of crystal water. However, the second process was through the wide temperature range 260 and 400 °C, and reached the greatest loss at 274 °C with a mass loss percentage of 58.2%, perhaps because of the decomposition of the ligands. Furthermore, it is concluded through the thermal decomposition mechanism that the final residue may be mixtures of zinc oxide and its polymer.

From the DSC and TG-DTG curves, thermal decomposition of four complexes with DATr as ligands first have loss of water, then phase change, and at last exothermic decomposition process. Complex **2** is more stable than the other three complexes, whereas **4** has relatively poor stability. As a result of the similar properties compared to **2–4** and the elemental analysis, the structure of **1** is suggested as $Mn_3[(DATr)_6(H_2O)_6](NO_3)_6{\cdot}2H_2O$ (**1**).

Energy of combustion is a significant parameter to assess energetic properties of new complexes. Energies of combustion of the four complexes were surveyed in table 4. Constant volume energies of combustion (Q_v) were measured by oxygen bomb calorimetry in an oxygen atmosphere. The physicochemical properties of the title coordination compounds are also listed in table 4. The nitrogen content of these complexes is nearly 40% by weight and these complexes can release a large amount of heat in combustion.

3.3. *Nonisothermal kinetics analysis*

Kissinger's methods [46] and Ozawa's [47] methods are widely used to determine the Arrhenius equation for a given material. The Kissinger [equation (a)] and Ozawa equations [equation (b)] are as follows:

$$\ln \beta/{T_p}^2 = \ln[RA/E_a] - E_a/(RT_p) \tag{a}$$

$$\lg \beta = \lg[AE_a/RG(\alpha)] - 2.315 - 0.4567E_a/(RT_p) \tag{b}$$

T_p is the temperature (°C) at which the first exothermic peak occurs in the DSC curve; A is the pre-exponential factor (s^{-1}); E_a is the apparent activation energy ($kJ\,M^{-1}$); R is the gas constant ($8.314\ J\,K^{-1}\,M^{-1}$); β is the linear heating rate ($K\,min^{-1}$); and G (α) is the reaction-mechanism function.

Table 4. Physicochemical properties of **1–4**.

	Complex **1**	Complex **2**	Complex **3**	Complex **4**
T_p (°C)[a]	298.3	350.1	340.7	255.3
N (%)[b]	39.59	39.16	39.22	39.44
E ($kJ\,M^{-1}$)[c]	133.33	181.67	143.67	120.2
Q_v ($MJ\,kg^{-1}$)[d]	12.79	16.24	15.32	8.36

[a] Thermal decomposition/DSC main exothermic peak at the heat rate of 5 °C min^{-1}.
[b] Nitrogen content.
[c] Activation energy.
[d] Constant volume energy of combustion.

Based on the first exothermic peaks measured with four different heating rates of 5, 10, 15, and 20 °C min^{-1}, Kissinger and Ozawa methods were applied to investigate the kinetic parameters of **1–4**. From these data, the apparent activation energies E_K and E_O (E is the average value of E_K and E_O), pre-exponential factor A_K, linear correlation coefficients R_K and R_O were determined and are listed in table 5.

Accordingly, the Arrhenius Equation for the coordination compounds can be expressed as equations (1)–(4):

$$\ln k = 9.717 - 133.333 \times 10^3/(RT) \tag{1}$$

$$\ln k = 12.890 - 181.667 \times 10^3/(RT) \tag{2}$$

$$\ln k = 9.742 - 143.667 \times 10^3/(RT) \tag{3}$$

$$\ln k = 9.444 - 120.200 \times 10^3/(RT) \tag{4}$$

The above equations can be used to estimate rate constants of the initial thermal decomposition process of the four complexes. For the mentioned complexes, **2** has the largest activation energy, suggesting that it can be more stable.

3.4. *Sensitivities properties*

In order to evaluate the possibility of the four complexes to be used as energetic materials, the impact, friction, and flame sensitivities were measured according to the Chinese GJB Standard [48].

The sensitivity to impact stimuli was determined by applying standard staircase method and the results are reported in terms of height for 50% probability of explosion (H_{50}) of the sample. The samples of the four complexes (20 mg) were placed between two steel poles and hit with a 0.8 kg drop hammer. The highest height which is used for testing 50% probability of explosion is 150 cm. Friction sensitivities were determined with a MGY-1 pendular friction sensitivity apparatus by a standard procedure using 20 mg of the sample. The complexes were compressed between two steel poles with mirror surfaces at a pressure of

Table 5. The temperature of the first main exothermic peak at the different heating rates and chemical kinetics parameters.

		Complex **1**	Complex **2**	Complex **3**	Complex **4**
T_p (°C) value	5	298.3	350.1	340.7	255.3
	10	308.7	359.7	349.9	263.9
	15	315.3	365.2	358.4	272.6
	20	326.5	374.8	370.2	281.4
Kissinger's method					
E_K (kJ M^{-1})		132.0	181.1	142.3	119.0
ln A_k		9.717	12.890	9.742	9.444
R_K		0.9754	0.9789	0.9667	0.9791
Ozawa's method					
E_O (kJ M^{-1})		134.8	182.3	145.2	121.8
R_O		0.9786	0.9812	0.9710	0.9819

Table 6. The impact, friction and flame sensitive results of **1–4**.

	1	**2**	**3**	**4**
IS[a] (H_{50}) (cm)	Not fire	21.35	48.36	Not fire
FS[b]	0	88	0	0
Flame[c] (H_{50}) (cm)	28.35	19.34	Not fire	Not fire

[a] Height (cm) for 50% probability of explosion towards impact.
[b] The firing rate at 90° angle towards friction.
[c] 50 percent probability of explosion for flame stimuli.

1.96 MPa and subsequently hit with a 1.0 kg hammer at a 90° angle relative to the horizontal. Flame sensitivities were tested by a HGY-1 Pendulum apparatus. About 20 mg of the sample was compacted into a copper cap with a pressure of 39.2 MPa and afterwards ignited by a standard black powder pellet. The results are summarized in table 6.

In the four complexes, **2** is more sensitive to impact than the other complexes. But towards friction stimuli, most of the coordination complexes with DATr as ligands are insensitive. Complexes **3** and **4** show lower sensitivity for flame stimuli. In summary, compared to the others, **2** is more sensitive to external stimuli. However, **4** is most insensitive. Therefore, the coordination compounds based on DATr are moderately sensitive and handled with relative safety.

4. Conclusion

To develop environmentally compatible green energetic materials, four metal complexes (Mn(II),Co(II), Ni(II), and Zn(II)) based on DATrs as main ligands with nitrate anions as outer ions were synthesized and characterized. By single-crystal X-ray analyses, the crystal structures of **2**, **3**, and **4** consist of a trinuclear unit. The central metal ions are six-coordinate in distorted octahedral configurations, whereas the N1 and N2 of DATr form a bridging mode to link two adjacent metals.

DSC and TG-DTG analyses show that **1–4** are thermally resistant (decompose above 260 °C). Complex **2** is more stable than the other three complexes while the zinc complex has relatively poor stability. The results of the nonisothermal kinetic analysis demonstrated that the activation energy of **2** was biggest, which also indicated that cobalt complex was relatively more stable. Sensitivity tests reveal that **2** is more sensitive to external stimuli, while **4** cannot be ignited by impact, friction or flame stimulus. Complex **3** is sensitive towards impact and insensitive towards friction or flame, whereas **1** is sensitive to flame, not to impact, friction. The cobalt complex which is easy to prepare and safe to transport can be a candidate as an insensitive explosive.

The experimentally measured energies of combustion demonstrate that these complexes can release a large amount of heat in combustion, which indicates that the title complexes have good energetic performances.

In contrast to current energetic complexes, including inorganic salts, organic complexes and inorganic coordination compounds with metallic cations, the title complexes with nontoxic metal ions, and good thermal stability (similar to that of strontium complexes [49], and higher than that of FOX-7 complexes [50, 51]) will be promising alternatives for eco-friendly green energetic materials.

4.1. *X-ray data collection and structure refinement*

Single crystals with suitable dimensions were selected for X-ray diffraction analysis. The data collection was performed with a Rigaku AFC-10/Saturn 724 + CCD detector diffractometer with graphite-monochromated Mo K_α radiation (λ = 0.71073 Å) at 153(2) K with multiscan modes. A semi-empirical absorption correction was applied to the raw intensities [52]. The structures were solved by direct methods using SHELXS-97 (Sheldrick, 1990) [53] and refined by full-matrix least-squares on F^2 with SHELXL-97 [54]. All nonhydrogen atoms were obtained from the difference Fourier map and refined anisotropically. The hydrogens were obtained geometrically and treated by a constrained refinement.

Supplementary material

Crystallographic data (excluding structure factors) for the structures in this paper have been deposited with the Cambridge Crystallographic Data Center, CCDC, 12 Union Road, Cambridge CB21EZ, UK. Copies of the data can be obtained free of charge on quoting the depository number CCDC-959957 (for **2**), CCDC-991060 (for **3**) and CCDC-959958 (for **4**) (Fax:+44 1223 336 033; Email: deposit@ccdc.cam.ac.uk; http://www.ccdc.cam.ac.uk).

Funding

We gratefully acknowledge the financial support from the National Natural Science Foundation of China [grant number 10776002], and the project of State Key Laboratory of Science and Technology [grant number ZDKT12-03].

References

[1] M.B. Talawar, R. Sivabalan, T. Mukundan, H. Muthurajan, A.K. Sikder, B.R. Gandhe, A.S. Rao. *J. Hazard. Mater.*, **161**, 589 (2009).
[2] N. Fischer, T.M. Klapötke, J. Stierstorfer. *J. Energ. Mater.*, **29**, 61 (2011).
[3] J.M. Shreeve. *Inorg. Chem.*, **51**, 5305 (2012).
[4] N. Fischer, D. Izsák, T.M. Klapötke, J. Stierstorfer. *Chem. - Eur. J.*, **19**, 8948 (2013).
[5] G.H. Tao, D.A. Parrish, J.M. Shreeve. *Inorg. Chem.*, **51**, 5305 (2012).
[6] S. Cudzilo, M. Nita. *J. Hazard. Mater.*, **177**, 146 (2010).
[7] Y. Cui, J. Zhang, T. Zhang, L. Yang, J. Zhang, X. Hu. *J. Hazard. Mater.*, **160**, 45 (2008).
[8] M. Joas, T.M. Klapötke, N. Szimhardt. *Eur. J. Inorg. Chem.*, **2014**, 493 (2014).
[9] C. Pettinari, F. Marchetti, S. Orbisaglia, J. Palmucci, R. Pettinari, C. Di Nicola, B.W. Skelton, A.H. White. *Eur. J. Inorg. Chem.*, **2014**, 546 (2014).
[10] M.A. Ilyushin, I.V. Tselinsky, A.Y. Zhilin, I.A. Ugryumov, A.V. Smirnov, A.S. Kozlov. *Chin. J. Energ. Mater.*, **12**, 15 (2004).
[11] Q. Yang, S. Chen, G. Xie, S. Gao. *J. Coord. Chem.*, **65**, 2584 (2012).
[12] Q. Zhang, J.M. Shreeve. *Angew. Chem. Int. Ed.*, **53**, 2540 (2014).
[13] S. Li, Y. Wang, C. Qi, X. Zhao, J. Zhang, S. Zhang, S. Pang. *Angew. Chem. Int. Ed.*, **52**, 1 (2013).
[14] Y.-C. Li, C. Qi, S.-H. Li, H.-J. Zhang, C.-H. Sun, Y.-Z. Yu, S.-P. Pang. *J. Am. Chem. Soc.*, **132**, 12172 (2010).
[15] C. Qi, S.-H. Li, Y.-C. Li, Y. Wang, X.-K. Chen, S.-P. Pang. *J. Mater. Chem.*, **21**, 3221 (2011).
[16] V. Thottempudi, J.M. Shreeve. *J. Am. Chem. Soc.*, **133**, 19982 (2011).
[17] M.M. Dirtu, C. Neuhausen, A.D. Naik, A. Rotaru, L. Spinu, Y. Garcia. *Inorg. Chem.*, **49**, 5723 (2010).
[18] K. Karaghiosoff, T.M. Klapötke, C. Miró Sabaté. *Chem. - Eur. J.*, **15**, 1164 (2009).
[19] T. Fendt, N. Fischer, T.M. Klapotke, J. Stierstorfer. *Inorg. Chem.*, **50**, 1447 (2011).
[20] D. Fischer, T.M. Klapötke, D.G. Piercey, J. Stierstorfer. *J. Energ. Mater.*, **30**, 40 (2012).
[21] A.Yu. Zhilin, M.A. Ilyushin, I.V. Tselinskii, A.S. Kozlov, I.S. Lisker. *Russ. J. Appl. Chem.*, **76**, 572 (2003).
[22] Z.-M. Li, T.-L. Zhang, G.-T. Zhang, Z.-N. Zhou, L. Yang, J.-G. Zhang, K.-B. Yu. *J. Coord. Chem.*, **66**, 1276 (2013).

[23] B.-D. Wu, J.-G. Zhang, T.-L. Zhang, L. Yang, Z.-N. Zhou. *Eur. J. Inorg. Chem.*, **2012**, 1261 (2012).
[24] M.B. Talawar, A.P. Agrawal, S.N. Asthana. *J. Hazard. Mater.*, **120**, 25 (2005).
[25] R. Sivabalan, M. Anniyappan, S.J. Pawar, M.B. Talawar, G.M. Gore, S. Venugopalan, B.R. Gandhe. *J. Hazard. Mater.*, **137**, 672 (2006).
[26] B.-D. Wu, S.-W. Wang, L. Yang, T.-L. Zhang, J.-G. Zhang, Z.-N. Zhou, K.-B. Yu. *Eur. J. Inorg. Chem.*, **2011**, 2616 (2011).
[27] L. Yi, B. Ding, B. Zhao, P. Cheng, D.-Z. Liao, S.-P. Yan, Z.-H. Jiang. *Inorg. Chem.*, **43**, 33 (2004).
[28] M.A. Ilyushin, I.V. Tselinskiy, A.V. Smirnov, I.V. Shugalei. *Cent. Eur. J. Energ. Mater.*, **9**, 3 (2012).
[29] D. Izsák, T.M. Klapötke, S. Reuter, T. Rösener. *Z. Anorg. Allg. Chem.*, **639**, 899 (2013).
[30] N. Segaud, J.N. Rebilly, K. Senechal-David, R. Guillot, L. Billon, J.P. Baltaze, J. Farjon, O. Reinaud, F. Banse. *Inorg. Chem.*, **52**, 691 (2013).
[31] J. Kerth, S. Lobbecke. *Propell. Explos. Pyrot.*, **27**, 111 (2002).
[32] B.-D. Wu, F.-G. Li, T.-L. Zhang, L. Yang, Z.-N. Zhou, J.-G. Zhang. *Z. Anorg. Allg. Chem.*, **639**, 1248 (2013).
[33] M.H.V. Huynh, M.A. Hiskey, E.L. Hartline, D.P. Montoya, R. Gilardi. *Angew. Chem.-Int. Ed.*, **43**, 4924 (2004).
[34] B.-D. Wu, Y.-G. Bi, Z.-N. Zhou, L. Yang, J.-G. Zhang, T.-L. Zhang. *J. Coord. Chem.*, **66**, 3014 (2013).
[35] S. Cudziło, W. Trzciński, M. Nita, S. Michalik, S. Krompiec, R. Kruszyński, J. Kusz. *Propell. Explos. Pyrot.*, **36**, 151 (2011).
[36] S.-W. Wang, L. Yang, J.-L. Feng, B.-D. Wu, J.-G. Zhang, T.-L. Zhang, Z.-N. Zhou. *Z. Anorg. Allg. Chem.*, **637**, 2215 (2011).
[37] P.N. Gaponik, S.V. Voitekhovich, A.S. Lyakhov, V.E. Matulis, O.A. Ivashkevich, M. Quesada, J. Reedijk. *Inorg. Chim. Acta*, **358**, 2549 (2005).
[38] Y.H. Joo, B. Twamley, S. Garg, J.M. Shreeve. *Angew. Chem.-Int. Ed.*, **47**, 6236 (2008).
[39] Q. Yang, Q. Wei, S.-P. Chen, G.-C. Zhang, C.-S. Zhou, S.-L. Gao. *J. Anal. Appl. Pyrolysis*, **99**, 66 (2013).
[40] S. Qi, Z. Li, Z. Zhou, Y. Cui, G. Zhang, T. Zhang, J. Zhang, L. Yang. *Chin. J. Chem.*, **29**, 59 (2011).
[41] T.M. Klapötke, C.M. Sabaté. *Cent. Eur. J. Energ. Mater.*, **7**, 161 (2010).
[42] I.S. Konovalova, S.V. Shishkina, B.V. Paponov, O.V. Shishkin. *CrystEngComm*, **12**, 909 (2010).
[43] I.S. Konovalova, Y.V. Nelyubina, K.A. Lyssenko, B.V. Paponov, O.V. Shishkin. *J. Phys. Chem. A*, **115**, 8550 (2011).
[44] A.D. Naik, B. Tinant, A. Léonard, J. Marchand-Brynaert, B.-L. Su, Y. Garcia. *Cryst. Growth Des.*, **11**, 4034 (2011).
[45] J.-T. Wu, J.-G. Zhang, X. Yin, M. Sun, T.-L. Zhang. *Z. Anorg. Allg. Chem.*, **639**, 2354 (2013).
[46] H.E. Kissinger. *Anal. Chem.*, **29**, 1702 (1957).
[47] T. Ozawa. *Bull. Chem. Soc. Jpn.*, **38**, 1881 (1965).
[48] Z.-T. Liu, Y.-L. Lao. *Initiation Explosive Experimental*, Beijing Institute of Technology, Beijing (1995).
[49] X.-B. Zhang, Y.-H. Ren, W. Li, F.-Q. Zhao, J.-H. Yi, B.-Z. Wang, J.-R. Song. *J. Coord. Chem.*, **66**, 2051 (2013).
[50] Z. Gao, J. Huang, K.-Z. Xu, W.-T. Zhang, J.-R. Song, F.-Q. Zhao. *J. Coord. Chem.*, **66**, 3572 (2013).
[51] F. He, K.-Z. Xu, H. Zhang, Q.-Q. Qiu, J.-R. Song, F.-Q. Zhao. *J. Coord. Chem.*, **66**, 845 (2013).
[52] G.M. Sheldrick. *SADABS*, University of Göttingen, Germany (1996).
[53] G.M. Sheldrick. *SHELXS-97, Program for the Solution of Crystal Structure*, University of Göttingen, Germany (1990).
[54] G.M. Sheldrick. *SHELXL-97, Program for the Solution of Crystal Structure*, University of Göttingen, Germany (1997).